Desalination and Water Treatment
www.deswater.com

doi: 10.5004/dwt.2019.23687

144 (2019) 257–262
March

The synthesis of a nano-Fe@NdFeB/AC magnetic catalyst and its application in the degradation of dimethyl phthalate by a Fenton-like process

Chunwei Yang[a,b,*], Baixiang Ren[a,b,*], Dong Wang[c], Qiang Tang[a,b]

[a]*Key Laboratory of Environmental Materials and Pollution Control, Education Department of Jilin Province, Jilin Normal University, Siping, China, Tel. +13694001402; email: chunwei_yang@jlnu.edu.cn (C. Yang), Tel. +86 13694001403; email: m13351582526@163.com (B. Ren), Tel. +13844406327; email: tangqian327@163.com (Q. Tang)*
[b]*College of Environmental Science and Engineering, Jilin Normal University, Siping, Jilin, China*
[c]*School of Environmental Science and Technology, Dalian University of Technology, Dalian, China, Tel. +13940950507; email: wangdong@dlut.edu.cn*

Received 28 June 2018; Accepted 25 December 2018

ABSTRACT

The heterogeneous catalytic Fenton-like process was selected in this study to degrade a dimethyl phthalate (DMP) solution. To enhance the efficiency and catalytic recycling ratio, a novel magnetic catalyst (nano-Fe loading on NdFeB magnetic activated carbon, Nano-Fe@NdFeB/AC) was synthesized. The results indicated that on the catalytic surface, globular Fe^0 has a size from 25 to 300 nm. This catalytic surface has sufficient magnetism to be separated by a magnetic separation method, in which the specific saturation magnetization and residual magnetization were 1.48 and 0.26 emu/g, respectively. At the optimal conditions of $[pH]_0 = 3.000$, $[H_2O_2]_0 = 4.24$ mmol/L, and $[\text{Nano-Fe@NdFeB/AC}]_0 = 5.0$ mg/L, the chemical oxygen demand removal ratio reached 85.2% after 120 min of reaction. The intermediate products monomethyl phthalate, phthalic acid, benzoquinone, hydroquinone, malonic acid, and oxalic acid were observed during the reaction. The DMP degradation was confirmed to be a hybrid mechanism of degreasing, acidification, and ring-opening reactions. The $^\bullet OH$ addition and oxidation in the aqueous phase represent the key degradation process, even though catalytic surface reactions occur at the same time. This system provides a new method to treat degradation-resistant pollution.

Keywords: Magnetic catalyst; Fenton-like; dimethyl phthalate; Heterogeneous catalytic reaction

---

1. Introduction

Dimethyl phthalate (DMP) has been widely used in plastic product production as a plasticizer because of its high solubility and stable chemical properties [1]. However, when DMP is present in the environment, it can lead to a series of problems because the compound is a typical endocrine disrupting chemicals (EDCs) [2]. Therefore, DMP in the wastewater must be destroyed before it was discharged. Additionally, it is hard for conventional biological processes to treat DMP efficiently [3,4]. Compared with biological wastewater treatment processes, advanced oxidation processes (AOPs), which have advantages of high reaction rate, low secondary pollution risk, and exhaustive mineralization, are more appropriate [5,6]. The Fenton process is the most commonly used AOP in China because it is simple, efficient, and safe [7]. However, there is plenty of iron sludge that has reportedly been disposed by traditional sludge treatment [8]. Furthermore, the acidic conditions will result in higher costs due to pH adjustment [9]. Therefore, a Fenton-like process that utilizes heterogeneous catalysts causes concerns [10,11]. To solve the problems of difficult separation and recycling, the catalyst has been given magnetism by doping Fe_3O_4 [12,13] and other magnetic particles [14]. NdFeB has wonderful

---

* Corresponding authors.

1944-3994/1944-3986

magnetic character and has been used in a preliminary study [15]. However, NdFeB was reactive in the aqueous phase and could result in diminished compound amounts and magnetism after a few reaction cycles. In this study, nano-Fe was loaded onto the surface of magnetic, NdFeB activated carbon (AC) (NdFeB/AC), and the chance of NdFeB reacting with water was minimized. On the other hand, the Fe^0 also has the ability to perform reductive dechlorination, catalytic ozonation, activation of peroxysulfate, and microelectrolysis with AC. Therefore, the novel Nano-Fe@NdFeB/AC magnetic catalyst may be an inexpensive and efficient solution to treat most organic water pollutants.

2. Materials and methods

2.1. Synthesis

NdFeB magnetic activated carbon (NdFeB/AC) was synthesized by a negative pressure spraying method that has been previously reported [15]. Nano-Fe^0 was obtained as follows: 1.000 g $FeSO_4{\cdot}7H_2O$ (AR. 99%) and 10 mL ethyl alcohol (AR. 99%) were added to 100 mL ultrapure water, and then added 20% (M/M) NaBH4 (AR. 99%) solution dropwise while stirring with an electric mixer (300 r/min). When the black particles (Nano-Fe^0) were observed, more $NaBH_4$ solution was dropped until the formed bubbles disappeared. Then, NdFeB/AC was added into the nano-Fe^0 solution while stirring (70 rpm) for 10 min. Next, particles were separated with a magnet and dried in a furnace at room temperature (25°C) under N_2 protection. Finally, nano-Fe@NdFeB/AC was obtained.

2.2. Characterization

The morphology and structures of the catalyst were observed by a scanning electron microscope (SEM, S-570, Hitachi, Japan). The crystal phases of the obtained catalyst were characterized by X-ray powder diffraction (XRD, D/max-2500/PCX, Rigaku, Japan). The magnetism of the catalyst was tested by a vibrating sample magnetometer (VSM, 7407, Lakeshore, USA). The chemical oxygen demand (COD) of the DMP solution was measured by a COD analyzer (HI839800, HANA, Italy). The intermediate products were determined by high performance liquid chromatography (HPLC) (LC-6A, Shimadzu, Japan) and gas chromatography-mass spectrometry (GC-MS) analyses (GCMS-QP2010, Shimadzu). The pH values were obtained using a pH analyzer (pHS-26, Rex Electric Chemical, China).

2.3. DMP degradation by Fenton-like process

The DMP degradation reaction was carried out in a beaker. An electric mixer (75 rpm/min) was used during the reaction. DMP at an initial concentration of 5 mg/L was selected as the model for organic pollution. After pH adjustment of the solution by H_2SO_4 (10% M/M) and NaOH (5% M/M), a certain concentration of Nano-Fe@NdFeB/AC and H_2O_2 was added. At setting reaction time, samples were taken and adjusted to pH 9.000. Intermediate products were analyzed after sample filtration using a 0.45-μm filter membrane. The COD of the samples was measured after the samples were added MnO_2 (0.1 mmol/L) and placed for 24 h at room temperature (25°C). The morphology, elementary composition, and magnetism of Nano-Fe@NdFeB/AC were also studied.

3. Results and discussion

3.1. The characteristics of Nano-Fe@NdFeB/AC

The SEM results of the obtained catalytic Nano-Fe@NdFeB/AC are shown in Fig. 1. The AC has a porous structure, and the surface is relatively smooth, with large holes. The equivalent diameter of the large holes ranges from 1 to 10 μm, as shown in Fig. 1(a). Fig. 1(b) shows that NdFeB particles are present inside the large AC holes, and Fig. 1(c) shows that Fe^0 is also present within the large holes or adheres to the AC surface. The Fe^0 has a globular appearance, and the size ranges from 25 to 300 nm.

The XRD results are shown in Fig. 2. The XRD pattern of Nano-Fe@NdFeB/AC has obvious differences at 45° and 40°–50°, which are the Fe^0 and $Nd_2Fe_{14}B$ peaks, respectively. The pattern from 20° to 30° is attributed to the amorphous carbon peaks of AC. The peak at 35° is attributed to NdFeB. Therefore, NdFeB (or $Nd_2Fe_{14}B$) and Fe^0 were successfully loaded on the AC as expected.

The magnetism of catalytic Nano-Fe@NdFeB/AC was also evaluated, and the hysteresis loops are shown in Fig. 3. The VSM results indicated that the catalyst has typical hard magnetic characteristics. The specific saturation magnetization and residual magnetization of the catalyst were 1.48 and 0.26 emu/g, respectively. The coercivity reached 185.51 Oe. This catalyst can easily be reused by a magnetic separation technique.

3.2. Optimal conditions of DMP degradation by a Fenton-like process

In this study, the conditions of the initial H_2O_2 concentration ($[H_2O_2]_0$), catalyst doses ($[\text{Nano-Fe@NdFeB/AC}]_0$), and initial pH ($[pH]_0$) were investigated to obtain the optimal conditions for DMP COD removal. The $[H_2O_2]_0$ is a key factor in organic pollution degradation, and the results of the influence of $[H_2O_2]_0$ are shown in Fig. 4(a). Under the conditions of $[DMP]_0$ = 5 mg/L, $[pH]_0$ = 3.000, and $[\text{Nano-Fe@NdFeB/AC}]_0$ = 10 mg/L, at room temperature, the COD removal ratios were increased rapidly in 10 min and became steady after 20 min. The COD removal ratio was influenced by $[H_2O_2]_0$. After 120 min of reaction, the COD removal ratio increased from 49.2% to 70.7% when $[H_2O_2]_0$ increased from 1.06 to 4.24 mmol/L. However, when $[H_2O_2]_0$ increased to 5.30 mmol/L, the COD removal ratio decreased to 58.6%. This result is because H_2O_2 can decompose to hydroxyl radicals (•OH), which are the key free radicals on organic degradation in the Fenton process. Increased •OH levels mean that more organic pollutants can be degraded [shown in Eqs. (1) and (2)] [16]. However, when $[H_2O_2]_0$ increases up to 5.30 mmol/L, the •OH concentration will rapidly grow and side reactions will also be intensified, which will impede the COD decline [shown in Eqs. (3) and (4)] [17]. These results are consistent with those of other reports [18,19]. In this study, the optimal $[H_2O_2]_0$ to degradation DMP is 4.24 mmol/L.

$$Fe^{2+} + H_2O_2 \rightarrow Fe^{3+} + OH^- + {}^\bullet OH \quad (1)$$

$$Fe^{3+} + H_2O_2 \rightarrow Fe^{2+} + HO_2^\bullet + H^+ \quad (2)$$

$${}^\bullet OH + {}^\bullet OH \rightarrow H_2O_2 \quad (3)$$

$${}^\bullet OH + H_2O_2 \rightarrow HO_2^\bullet + H_2O \quad (4)$$

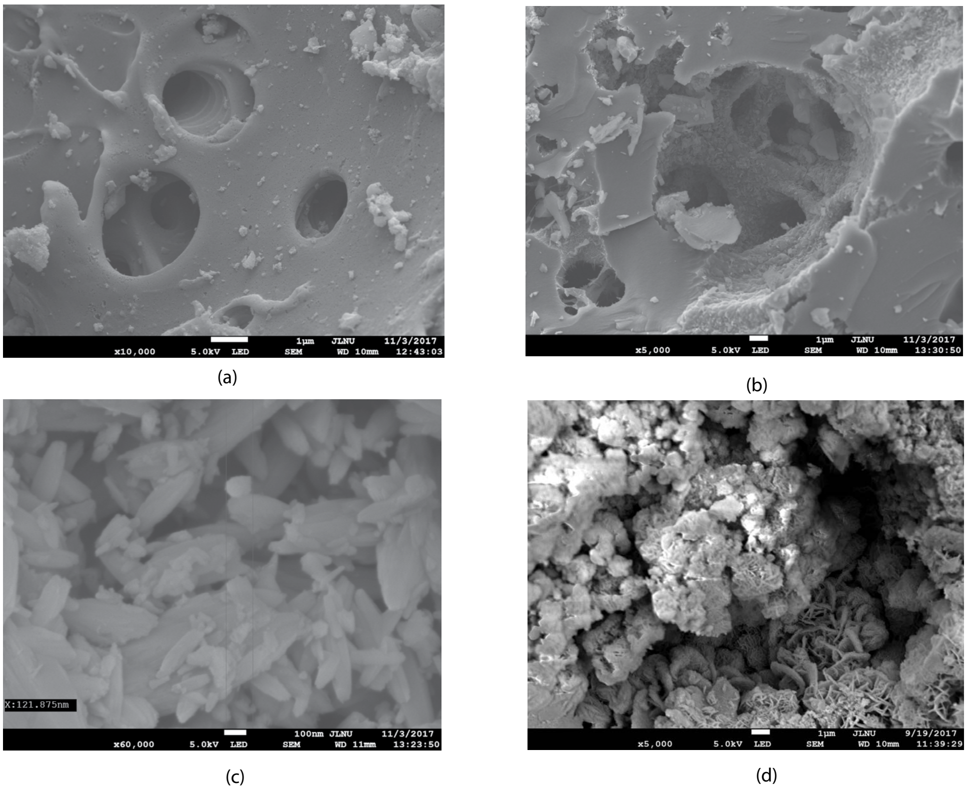

(a) (b) (c) (d)

Fig. 1. SEM results of AC (a), Nano-Fe@NdFeB/AC (b, c), and Nano-Fe@NdFeB/AC (after 3 cycle reactions) (d).

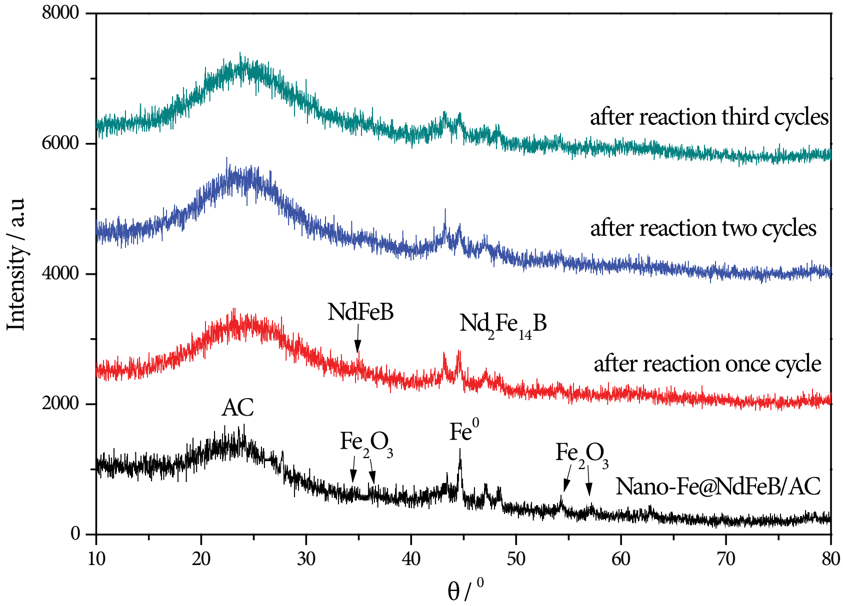

Fig. 2. XRD results of Nano-Fe@NdFeB/AC and Nano-Fe@NdFeB/AC (after reaction).

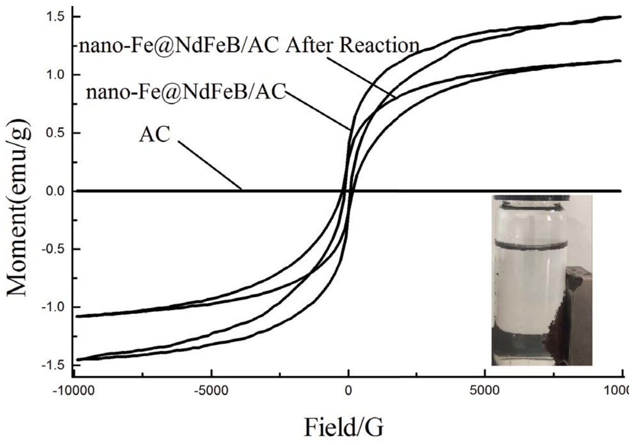

Fig. 3. VSM results of AC, Nano-Fe@NdFeB/AC, and Nano-Fe@NdFeB/AC (after 3 cycle tests). The photo inlet was the Nano-Fe@NdFeB/AC (after 3 cycle tests) separated from water by a magnet.

The catalyst dose also has optimal conditions, as shown in Fig. 4(b). It was found that 5 mg/L is the suitable dose for COD removal, which could reach 82.8% after 120 min of treatment under the conditions of $[DMP]_0$ = 5 mg/L, $[pH]_0$ = 3.000, and $[H_2O_2]_0$ = 4.24 mmol/L at room temperature. When the catalyst dose was down to 2.5 mg/L, the COD removal ratio was only 52.8%. However, when the catalyst dose reached 10.0, 15.0, 20, and 25 mg/L, the COD removal ratio was 70.7%, 70.6%, 70.2%, and 70.1%, respectively. Higher or lower catalyst dose can lead to a decrease in the COD removal ratio. This decrease is because more catalyst can activate more H_2O_2 to generate $^{\bullet}$OH when the catalyst dose is low. However, when the catalyst dose is too high, the possibility of side reactions [Eq. (5)] [20] will also be enhanced, and the $^{\bullet}$OH concentrations will not increase and even may decline.

$$\bullet OH + Fe^{2+} \rightarrow Fe^{3+} + OH^- \tag{5}$$

A previous study indicated that pH is also very important to the Fenton process. The impact of pH on the COD removal ratio was also determined, and the results are shown in Fig. 4(c). Under the conditions of $[DMP]_0$ = 5 mg/L, $[H_2O_2]_0$ = 4.24 mmol/L, and $[\text{Nano-Fe@NdFeB/AC}]_0$ = 5 mg/L, the optimal pH value is 3.000 and the COD removal ratio reaches 85.2%, which is higher than the ratios of 71.6% for pH 2.000, 68.2% for pH 4.000, and 55.3% for pH 5.000. Both higher and lower pH values have negative effects on DMP degradation. For the homogeneous Fenton process, Eq. (1) confirms that the lower pH condition is beneficial to $^{\bullet}$OH generation. When the pH is too low, the reduction of Fe^{3+} to Fe^{2+} reaction will be hampered [Eqs. (6) and (7)] [21]. However, a higher pH value may cause Fe^{2+} and Fe^{3+} to generate precipitates, and the catalytic efficiency will decrease rapidly. However, for a heterogeneous Fenton-like process, the catalytic surface has active sites that can promote catalytic and oxidation reactions. Therefore, in this study, even at pH = 6.000, the COD removal ratio also reached 53.2%. However, the efficiency decrease following pH variation indicated that most DMP degradation reactions were homogeneous reactions occurring in the solution. The heterogeneous catalytic and oxidation reactions are not the main contributors.

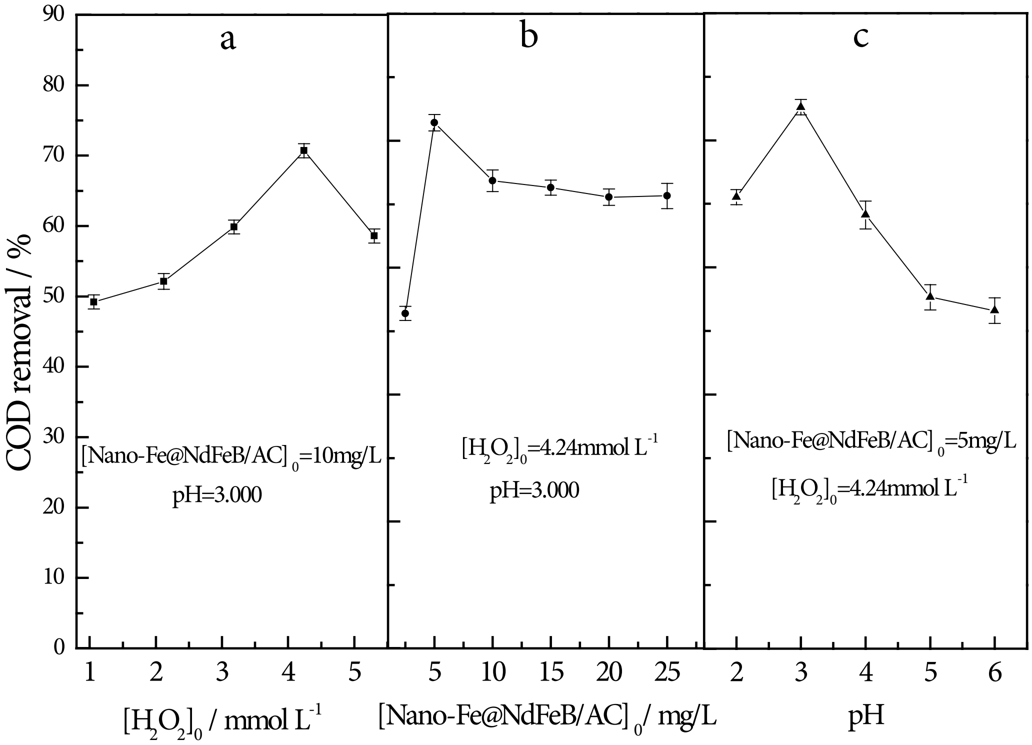

Fig. 4. The optimal condition of DMP degradation by Fenton-like process.

$$Fe^{3+} + H_2O_2 \rightarrow Fe^{2+} + HO_2^{\bullet} + H^+ \quad (6)$$

$$Fe^{3+} + HO_2^{\bullet} \rightarrow Fe^{2+} + H^+ + O_2 \quad (7)$$

Consecutive cycle tests of DMP degradation by the Fenton-like process with Nano-Fe@NdFeB/AC as a heterogeneous catalyst were carried out, and the results are shown in Fig. 5. The COD removal ratio could be maintained at nearly 80% in the test with three consecutive cycles under the conditions of $[DMP]_0$ = 5 mg/L, $[H_2O_2]_0$ = 4.24 mmol/L, and $[\text{Nano-Fe@NdFeB/AC}]_0$ = 5 mg/L at room temperature.

3.3. Possible mechanisms

To assess the mechanism of DMP degradation with Nano-Fe@NdFeB/AC as the heterogeneous catalyst, the serial tests were carried out. The morphology, crystal phases, and magnetism of Nano-Fe@NdFeB/AC were measured following catalysis with H_2O_2 to degrade DMP after one, two, and three cycles. Fig. 1(d) shows that the catalyst surface became fluffy after the reaction. The amounts of nano-Fe on the catalyst surface decreased after the reaction, and a longer reaction time led to less nano-Fe observed (Fig. 2). This result is because during the reaction, nano-Fe on the surface could react and generate Fe^{2+}, which could dissolve into solution. However, based on the XRD results (Fig. 2), Fe_3O_4 and Fe_2O_3 were also observed on the surface of the catalyst. Therefore, the fluffy surface of the catalyst could be composed of Fe^{2+} and Fe^{3+} oxides. Even though the dissolution reaction was verified, the nano-Fe was also observed, based on the XRD results. Furthermore, the fluffy surface is beneficial to the organic pollutant adsorption. The VSM results indicated that after 3 reaction cycles (Fig. 3), the specific catalytic saturation magnetization and residual magnetization were 1.13 and 0.26 emu/g, respectively. The coercivity could reach 138.14 Oe. This catalyst could also be easily separated by a magnetic separation process even after the reaction (Fig. 3 inlet photo).

Consecutive cycle tests of Nano-Fe@NdFeB/AC-activated Fenton-like process DMP degradation were carried out, and the results are shown in Fig. 5. The COD removal ratio could reach 80% in three consecutive test cycles under the conditions of $[pH]_0$ = 3.000, $[H_2O_2]_0$ = 4.24 mmol/L, and $[\text{Nano-Fe@NdFeB/AC}]_0$ = 5.0 mg/L.

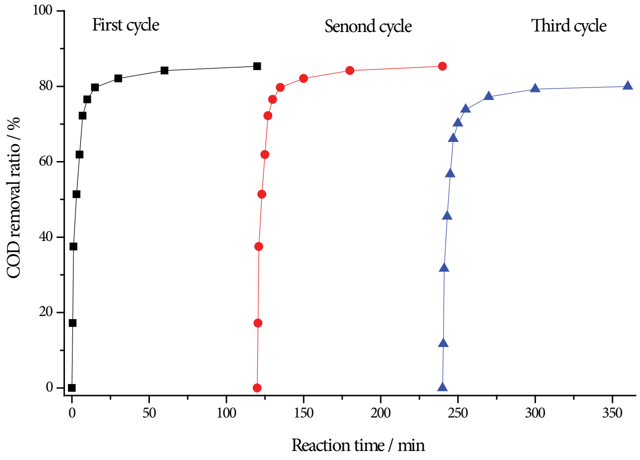

Fig. 5. Results of consecutive cycles of DMP degradation tests.

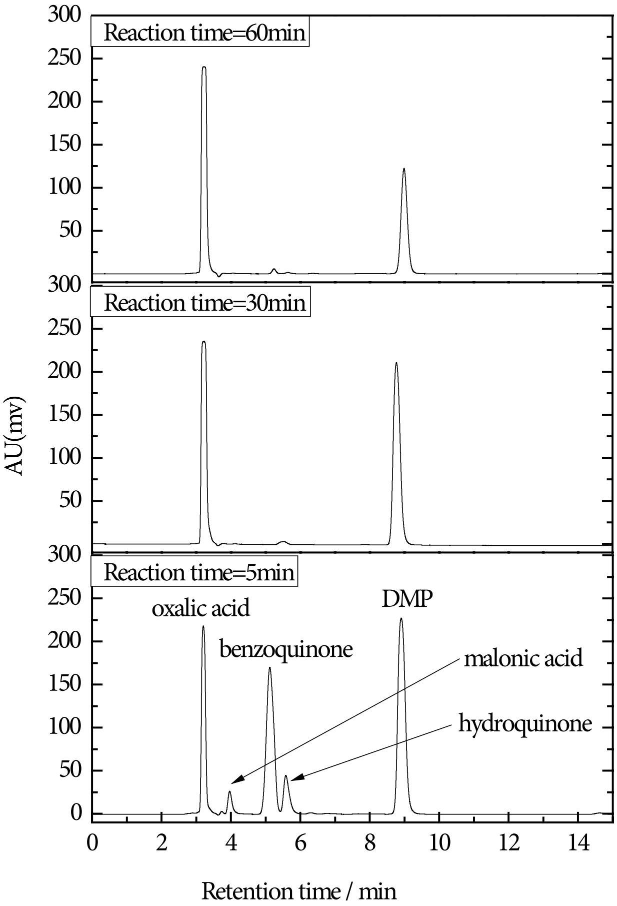

Fig. 6. HPLC results of DMP degradation by Fenton-like process.

The intermediate products during the reaction (5, 30, and 60 min) were analyzed by HPLC (Fig. 6). Benzoquinone, hydroquinone, malonic acid, and oxalic acid were observed after the 5-min reaction. However, for samples of 30 and 60 min reaction times, only DMP, oxalic acid, and some benzoquinone were identified. The intermediate products of benzoquinone and hydroquinone indicated that $^{\bullet}OH$ was the key oxidizer during DMP degradation. GC-MS was also used to confirm the volatile intermediate products. Monomethyl phthalate and phthalic acid were found. Therefore, the ester groups in DMP were first oxidized to acid groups, followed by $^{\bullet}OH$ addition and ring-opening reactions.

4. Conclusion

A novel magnetic catalyst Nano-Fe@NdFeB/AC was prepared to promote the Fenton-like degradation of a DMP solution. This catalyst has satisfactory magnetism and good degradation performance on the model pollutant DMP, even when using 3 consecutive cycles. Under optimal conditions of $[pH]_0$ = 3.000, $[Na_2S_2O_8]_0$ = 4.24 mmol/L, and $[\text{Nano-Fe@NdFeB/AC}]_0$ = 5.0 mg/L, the COD removal ratio could reach

80% after a 30-min reaction. The $^{\bullet}$OH addition and oxidation reactions in the aqueous phase represent the key degradation process, even though catalytic surface reactions also occur at the same time. The pathway of DMP degradation was confirmed, which involved degreasing, acidification, and ring-opening reactions.

Acknowledgements

This work was supported by the National Natural Science Foundation of China (Grant No. 51708250) and The Project of Department of Science & Technology of Jilin Province (20180623042TC).

References

[1] T. Wang, G. Qu, X. Yin, Q. Sun, D. Liang, X. Guo, H. Jia, Dimethyl phthalate elimination from micro-polluted source water by surface discharge plasma: performance, active species roles and mechanisms, J. Hazard. Mater., 357 (2018) 279–288.

[2] Y. Wang, Y. Liu, T. Liu, S. Song, X. Gui, H. Liu, P. Tsiakaras, Dimethyl phthalate degradation at novel and efficient electro-Fenton cathode, Appl. Catal., B., 156–157 (2014) 1–7.

[3] T. Zhang, Z. Huang, X. Chen, M. Huang, J. Ruan, Degradation behavior of dimethyl phthalate in an anaerobic/anoxic/oxic system, J. Environ. Manage, 184 (2016) 281–288.

[4] J. Mo, Z. Wang, W. Xu, S. Li, Z. Yu, Enhanced production of dimethyl phthalate-degrading strain *Bacillus* sp. QD14 by optimizing fermentation medium, Electron. J. Biotechnol., 18 (2015) 244–251.

[5] Z. Wang, D. Deng, L. Yang, Degradation of dimethyl phthalate in solutions and soil slurries by persulfate at ambient temperature, J. Hazard. Mater., 271 (2014) 202–209.

[6] T. Wang, H. Jia, X. Guo, T. Xia, G. Qu, Q. Sun, X. Yin, Evaluation of the potential of dimethyl phthalate degradation in aqueous using sodium percarbonate activated by discharge plasma, Chem. Eng. J., 346 (2018) 65–76.

[7] Q. Zhou, Y. Liu, G. Yu, F. He, K. Chen, D. Xiao, X. Zhao, Y. Feng, J. Li, Degradation kinetics of sodium alginate via sono-Fenton, photo-Fenton and sono-photo-Fenton methods in the presence of TiO_2 nanoparticles, Polym. Degrad. Stab., 135 (2017) 111–120.

[8] F. Zhang, Q. Yue, Y. Gao, B. Gao, X. Xu, Z. Ren, Y. Jin, Application for oxytetracycline wastewater pretreatment by Fenton iron mud based cathodic-anodic-electrolysis ceramic granular fillers, Chemosphere, 182 (2017) 483–490.

[9] X. Wang, A. Wang, J. Ma, Visible-light-driven photocatalytic removal of antibiotics by newly designed C_3N_4@$MnFe_2O_4$-graphene nanocomposites, J. Hazard. Mater., 336 (2017) 81–92.

[10] H. Zhang, Z. Xiong, F. Ji, B. Lai, P. Yang, Pretreatment of shale gas drilling flowback fluid (SGDF) by the microscale Fe^0/persulfate/O_3 process (mFe^0/PS/O_3), Chemosphere, 176 (2017) 192–201.

[11] Z. Wan, J. Wang, Degradation of sulfamethazine using Fe_3O_4-Mn_3O_4/reduced graphene oxide hybrid as Fenton-like catalyst, J. Hazard. Mater., 324 (2017) 653–664.

[12] Y. Wang, X. Lin, Z. Shao, D. Shan, G. Li, A. Irini, Comparison of Fenton, UV-Fenton and nano-Fe_3O_4 catalyzed UV-Fenton in degradation of phloroglucinol under neutral and alkaline conditions: Role of complexation of Fe^{3+} with hydroxyl group in phloroglucinol, Chem. Eng. J., 313 (2017) 938–945.

[13] D. Wan, W. Li, G. Wang, L. Lu, X. Wei, Degradation of p-Nitrophenol using magnetic Fe^0/Fe_3O_4/Coke composite as a heterogeneous Fenton-like catalyst, Sci. Total Environ., 574 (2017) 1326–1334.

[14] L. Zhang, D. Xu, C. Hu, Y. Shi, Framework Cu-doped AlPO 4 as an effective Fenton-like catalyst for bisphenol A degradation, Appl. Catal., B, 207 (2017) 9–16.

[15] C. Yang, D. Wang, Q. Tang, The synthesis of NdFeB magnetic activated carbon and its application in degradation of azo dye methyl orange by Fenton-like process, J. Taiwan Inst. Chem. Eng., 45 (2014) 2584–2589.

[16] J.H. Shen, J.J. Horng, Y.S. Wang, Y.R. Zeng, The use of reactive index of hydroxyl radicals to investigate the degradation of acid orange 7 by Fenton process, Chemosphere, 182 (2017) 364–372.

[17] R. Pulicharla, S.K. Brar, T. Rouissi, S. Auger, P. Drogui, M. Verma, R.Y. Surampalli, Degradation of chlortetracycline in wastewater sludge by ultrasonication, Fenton oxidation, and ferro-sonication, Ultrason. Sonochem., 34 (2017) 332–342.

[18] J. Wang, C. Liu, J. Li, R. Luo, X. Hu, X. Sun, J. Shen, W. Han, L. Wang, In-situ incorporation of iron-copper bimetallic particles in electrospun carbon nanofibers as an efficient Fenton catalyst, Appl. Catal., B, 207 (2017) 316–325.

[19] J. Shi, T. Long, R. Ying, L. Wang, X. Zhu, Y. Lin, Chemical oxidation of bis(2-chloroethyl) ether in the Fenton process: kinetics, pathways and toxicity assessment, Chemosphere, 180 (2017) 117–124.

[20] N. Nordin, L.-N. Ho, S.-A. Ong, A.H. Ibrahim, Y.-S. Wong, S.-L. Lee, Y.-S. Oon, Y.-L. Oon, Hybrid system of photocatalytic fuel cell and Fenton process for electricity generation and degradation of Reactive Black 5, Sep. Purif. Technol., 177 (2017) 135–141.

[21] A. Mirzaei, Z. Chen, F. Haghighat, L. Yerushalmi, Removal of pharmaceuticals from water by homo/heterogonous Fenton-type processes - a review, Chemosphere, 174 (2017) 665–688.